JEE Journal of Ecological Engineering

Journal of Ecological Engineering, 2025, 26(8), 38–56
https://doi.org/10.12911/22998993/203528
ISSN 2299–8993, License CC-BY 4.0

Received: 2025.03.13
Accepted: 2025.05.26
Published: 2025.06.10

Novel green synthesis of titanium oxide using *Lansium domesticum* Correa for photocatalytic degradation of methyl orange

Deliza Deliza[1,2], Safni Safni[1*], Rahmiana Zein[1], Reza Audina Putri[3]

[1] Department of Chemistry, Faculty of Mathematics and Natural Sciences, Andalas University, Limau Manis, Padang, West Sumatera, 25163, Indonesia
[2] Department of Chemistry, Faculty of Science and Technology, UIN Sulthan Thaha Saifuddin, Jambi 36361, Indonesia
[3] Research Centre for Chemistry, National Research and Innovation Agency, Building 452 KST BJ Habibie, South Tangerang, Indonesia
* Corresponding author's e-mail: safni@sci.unand.ac.id

ABSTRACT

This paper presents an eco-friendly method to synthesize TiO_2 NPs using *Lansium domesticum* Correa fruit peel extract as a capping agent. A UV-Vis signal at 239 nm confirmed the role of the extract in synthesizing TiO_2 NPs, with XRD revealing a crystalline anatase TiO_2 phase. Rietveld refinement is used to analyze the precise structural characteristics of TiO_2 NPs and the acceptable model. FESEM showed spherical particles of 17.6 nm, and PSA indicated an average size of 43.3 nm. FTIR suggested that the phytochemicals of the peel extract be used as reducing and capping agents. The BET of TiO_2 NPs was 88.0470 m²/g, with a mean pore diameter of 15. 2281 nm and total pore volume of 0.2299 cm³/g, TiO_2 NPs exhibited 97.74% photocatalytic degradation of MO dyes, indicating potential for application. The present findings offer an eco-friendly and cost-effective method and highlight *Lansium domesticum* peel waste as a potential reducing and capping agent for synthesizing TiO_2 NPs for wastewater treatment applications. This research significantly contributes to advances in sustainable materials science and environmental engineering.

Keywords: eco-friendly synthesis, TiO_2, *Lansium domesticum*, methyl orange, photocatalysis, degradation.

INTRODUCTION

Industrial waste containing chemicals continues to be a concern regarding water pollution and public health (Rahimi et al., 2023). One of the culprits in this issue is dyes such as methyl orange (MO), commonly used in industries like textiles and printing (Li et al., 2013; Subha and Jayaraj, 2015). The durability and resistance to breakdown characterizing MO make it difficult to eliminate wastewater streams. As a result of this challenge, there is a growing demand for treatment methods. Dye pollutants can be treated using physical, chemical, biological, and hybrid methods. Chemical methods like oxidation, reduction, ozonation, Fenton, piezo catalysis (Bößl et al., 2021; Zhang et al., 2024), and photocatalysis are used for optimal removal and degradation, particularly in textile and dye manufacturing industries. Emerging processes like photocatalysis show promise in addressing wastewater dye pollution (Dalal et al., 2023). Titanium dioxide (TiO_2) photocatalysis is a recognized and efficient approach for breaking down harmful chemical compounds, which creates reactive oxygen species upon exposure to light. Researchers comprehend this phenomenon due to the current emphasis on investigating the management of synthetic dyes. Researchers have gained an understanding of this phenomenon due to the recent focus on studying the manipulation of synthetic dyes. For years there has been a focus on enhancing the photocatalytic capabilities of TiO_2 through the exploration of different dopants and composite materials like TiO_2-$NiFe_2O_4$, TiO_2-$CuFe_2O_4$, and TiO_2-$MnFe_2O_4$ (Deliza et al., 2014), as well as N-doped TiO_2 (Safni et al., 2015) and C-N-Codoped (Putri et al., 2020; Safni et al., 2015; Safni et al., 2016; Vanny et al., 2017). Consequently, researchers aim to continually develop and apply new knowledge to advance the novelty of this research over time. These research efforts have opened up the possibilities for advancements in photocatalysis technology. However, the conventional chemical approaches used for producing TiO_2 nanoparticles (TiO_2 NPs) tend to rely on the methods that often involve toxic chemicals (e.g., sodium hydroxide, titanium tetrachloride) and high energy requirements. That brings about health concerns and the environment. In contrast, biosynthesis uses plant extracts (Kaur et al., 2019; Wagutu et al., 2019) and microbes (Koopi and Buazar, 2018). Enzymes (Survase and Kanase, 2023) offers a greener alternative, maintaining the beneficial properties of TiO_2 NPs while minimizing environmental impact. The reports articulated herein are congruent with the assertions posited by Akritidis et al. (2022). While conventional methods have proven effective, the shift towards biosynthesis and other innovative techniques reflects a growing awareness of environmental sustainability in nanoparticle production.

Plant-based synthesis, in particular, has gained attention due to its simplicity, low cost, and ability to reduce environmental impacts (Legmairi et al., 2024). Phytochemicals in plants, such as alkaloids, flavonoids, phenolics, proteins, amino acids, saponins, terpenoids, and glycosides, act as reducing agents, converting metal ions (e.g., Ti^{4+} to TiO_2), while also stabilizing the nanoparticles. One notable example of this approach is the use of *Averrhoa carambola* leaf extract, which has been shown to produce TiO_2 NPs with a small crystalline size (40 nm) and pure anatase phase, demonstrating excellent photocatalytic degradation of organic pollutants such as Malachite Green (91%) and Rhodamine B (92%) under UV light (Prammitha Rajaram, Ambrose Rejo Jeice, 2023, 2024). This method not only contributes to environmental sustainability but also adds value to agricultural waste products (Buazar et al., 2016; Chanani and Buazar, 2023). Khallel et al. (2022) utilizing the *Pulicaria undulata* extract to synthesize TiO_2 NPs, their potential for photocatalytically degrading MO and methylene blue under UV-visible light irradiation was investigated. In a brief amount of time (between 1 and 2 hours), approximately 95% of the target degradation was achieved. Previous research has explored various plant extracts for the green synthesis of TiO_2 NPs, including *Aloe vera* (Srujana et al., 2022; Wellia et al., 2024), *Azadirachta indica* (Sankar, 2015), *Aegle marmelos* (Ahmad et al., 2021), *Citrus aurantifolia* (Vishali et al., 2021), *Trigonella foenum-graecum* (Subhapriya and Gomathippriya, 2018), *Moringa* (Patidar and Jain, 2017), *Curcuma longa*, and *Hibiscus rosa*-sinensis (Jalill et al., 2016). Additionally, *Annona squamosa* (Roopan, 2012), and *Parkia speciosa* (Khoiriah and Putri, 2024), (Abisharani et al., 2019; Aravind et al., 2023; Devikala et al., 2021), have been successfully used in this context. However, to date, there have been no reports on the use of *Lansium domesticum* Correa (commonly known as langsat or duku) fruit peel extract for the synthesis of TiO_2 NPs.

The peel of *Lansium domesticum* contains a rich array of phytochemicals, including triterpenoids, phenolics, and flavonoids, making it an ideal candidate for the green synthesis of TiO_2 NPs. These phytochemicals can act as natural reducing agents, promoting the formation of TiO_2 nanoparticles with potential applications in environmental remediation, particularly in the degradation of synthetic dyes like MO. This study aimed to synthesize and characterize TiO_2 NPs using *Lansium domesticum* fruit peel extract and to evaluate their effectiveness in the photocatalytic degradation of MO, offering a novel, eco-friendly approach to wastewater treatment (Ilyasu et al., 2024).

MATERIAL AND METHODS

Material

Titanium (IV) chloride solution ($TiCl_4$), 1.0 M in methylene chloride, Sigma-Aldrich), Methyl orange (Merck), and ammonia solution (NH_3, Merck, 25%) were used. Deionized water was consistently used throughout the experiment. Plant samples from the peel of *Lansium domesticum* were collected in Jambi province, Indonesia. Commercial anatase TiO_2 (Ishihara Sangyo, Ltd. Japan).

Phytochemical study of *Lansium domesticum* extract

Peel fruit of *Lansium domesticum* was obtained from Jambi, Indonesian. Qualitative analysis of the various phytochemicals present in the aqueous peel extract of *Lansium domesticum Correa* was carried out using a previously described protocol (Abdallah et al., 2022). Phytochemicals such as flavonoids, terpenoids, tannins, alkaloids, triterpenoids, and saponins were identified.

Preparation of peel fruit extract

The peel of *Lansium domesticum Correa* was sourced from Jambi, Indonesia, and its identification and authentication were conducted by the Herbarium at Andalas University (ANDA). The collected *Lansium domesticum Correa* material underwent a meticulous process: it was cut into small pieces, thoroughly cleaned using tap water and deionized water, and then left to air-dry in the shade for 4–6 days. The fruit peel of *Lansium domesticum Correa* is extracted by mixing the powder with distilled water in a beaker using the maceration method. The sample is heated to 60 °C for 10 minutes. It is then filtered using a funnel to separate the filtrate from the residue, measure the pH of the obtained filtrate, and collect it for the green synthesis of TiO_2. The voucher specimen was appropriately labeled, including detailed information about the treatment day and date. It can be seen in Figure 1.

Biosynthesis of TiO_2 NPs

The extract peel from the *Lansium domesticum Correa* was prepared by placing 10 grams of the fruit peel into an Erlenmeyer flask, along with deionized water. The mixture was then heated at 60 °C for 10 minutes. Following the heating process, the *Lansium domesticum Correa* peel extract was filtered using Whatman no. 1 (pore: 2.5 µm) and utilized for subsequent experiments, following the approach of the extract *Sargassum myriocystum* (Balaraman et al., 2022). Subsequently, 10 mL of this solution was added to $TiCl_4$ in a stirred solution of the peel extract, resulting in a color change from brown to light brown. The resulting mixture of *Lansium domesticum Correa* peel-synthesized TiO_2 NPs underwent centrifugation, followed by exposure to an oven for 10 hours at a temperature of 80 °C and a furnace for 2 hours at a temperature of 500 °C. Finally, the obtained nanoparticle was stored for future characterization and application.

Impact of radical scavengers

The experiments involve the capture of reactive oxygen. The generation of reactive oxygen species (ROS) was conducted during photocatalytic degradation by adding radical trapping reagents (scavengers). These tests followed the methods outlined by Putri et al. (2023) with slight modifications. In the study, 20 mM formic acid (FC), 10 mL isopropyl-alcohol (IPA), and 0.001 g

Figure 1. Synthesis process of TiO_2 NPs

benzoquinone (BQ) were used to examine hole (h^+), super-anion oxide ($O2^{\bullet-}$), and hydroxyl radicals (•OH), respectively, in 5 mg L^1 Methyl Orange solutions containing 0.01 g of NP TiO_2 catalyst and irradiated by UV light for 180 min. The control was the photocatalytic process without the addition of scavengers, which was used as a comparison.

Characterization of the synthesized TiO_2 NPs

UV-Vis spectra of TiO_2 NPs were analyzed (Genesys-20 Spectrophotometer). FT-IR was used to identify functional groups in TiO_2 NPs (Shimadzu IR Spirit). X-ray diffraction (XRD, PANalytical EMPYREAN diffractometer) was used to characterize the crystal and structure formation of the TiO_2 obtained. A field emission scanning electron microscope (FE-SEM with EDS, JEOL model 6390) was used to investigate particle size. Particle size analyzers were measured (PSA, HORIBA SZ-100 analyzer). BET and BJH analyses were carried out using a Quantachrome Nova 4200e instrument in order to determine the surface area and pore size characteristics of the TiO_2 NPs synthesized using green methods.

Photocatalytic degradation of MO

The produced TiO_2 NPs were used to photocatalytic degrade MO dye. The degradation tests were conducted in a photocatalytic reactor equipped with several types of light (UV-A lamp, UV-C lamp, visible light, solar light) serving as the light source for testing purposes with variation times 1–4 hours. In order to preserve the absence of light, the reactor setup was enclosed within a box and shielded with opaque black paper to prevent any interference from surrounding light sources. The on and off functions of the visible lamp were synchronized using a timer circuit to regulate the duration of the visible light exposure. A reactor with a concentration of 5 mg/L of MO, was combined with TiO_2 NPs. Following the treatment, the MO solution underwent centrifugation at a speed of 10,000 revolutions per minute for 10 minutes. The concentration of MO was measured with a UV-Vis spectrophotometer at a wavelength of 465 nm and then converted into a percentage to indicate the level of degradation. The study investigated several aspects that affect the photocatalysis process, including the light source, catalyst dosage, and initial concentration of MO.

$$\%\, dye\ degraded = \frac{OD1 - OD2}{OD1} \quad (1)$$

where: $OD1$ – absorbance before degradation,
$OD2$ – absorbance after degradation.

Table 1. Phytochemical constituents of peel extract *Lansium domesticum Correa*

Phytochemical	Observations
Alkaloids	+
Flavonoids	+
Phenolics	+
Saponins	+
Terpenoid	+
Steroid	-
Protein & Amino Acids	+
Glycosides	+

RESULTS AND DISCUSSION

Phytochemical analysis

The extract peel of *Lansium domesticum* was gathered and identified. The results of the phytochemical analysis of the aqueous peel extract are presented in Table 1. Triterpenoids are optically active compounds that affect light polarization on photocatalytic activity. Phenolic chemicals, which are potent antioxidants, can eliminate reactive oxygen species. *Lansium domesticum* peel extract contains polyphenolic components, such as gallic acid, which are reducing agents, while ellagic acid stabilizes the formation of metal oxide nanoparticle. Polyphenolic flavonoid molecules contribute electrons or hydrogen atoms, neutralize free radicals, and bind to metals. They attach to the surface of TiO_2 by coordinating electrons from their hydroxyl groups. They also decrease autoxidation and greatly reduce intracellular reactive oxygen species.

In this paper, *Lansium domesticum* peel extract as a bioreducing and capping agent was successfully used to synthesize TiO_2 NPs. The bioreduction of Ti ions and the capping of TiO_2 NPs are probably due to the various phytochemical compounds present in the peel extract. TiO_2 NP formation was indicated by color change from transparent to dark brown after 2 h incubation (Figure 2) and finally to white after calcination (Figure 1). This matter followed the methods outlined by Buazer et al. (2016) with slight modifications (Khalafi et al., 2019).

The gallic acid in *Lansium domesticum Correa* peel extract likely acts as a reducing agent by donating electrons to titanium hydroxide species, thereby converting Ti (IV) to Ti (III). Through redox interactions with oxygen from the environment, reduced titanium species form nuclei and develop into TiO_2 NPs. Nucleation and growth mechanisms depend on reaction circumstances.

UV-Vis spectroscopy

The initial evidence of TiO_2 NPs production was seen when the reaction mixture transitioned from colorless to light brown (Sepahvand et al., 2020). The phytochemicals of the water extract reduced TiO_2 molecules into nanoparticles, resulting in the development of a light brown to brown-white color perhaps due to surface plasmon vibrations excitation (Figure 2). The absorption spectra of the *Lansium domesticum* peel extract were measured by reducing TiO_2 NPs and recording it over wavelengths from 200 to 800 nm (Figure 3). The signal seen at 239 nm indicated polyphenols, natural compounds in plants that act as antioxidants that help the synthesis process of TiO_2 NPs. Previous studies have shown that such color changes can often confirm the formation of nanoparticles. Correspondingly, the observed UV–vis spectrum exhibited a pronounced absorbance peak at a wavelength of 239 nm, indicating the successful synthesis of TiO_2 NPs using *Lansium domesticum* extract peel (Figure 3). (Srinivasan, 2019).

XRD analysis

The XRD pattern showed peaks with 2θ values of about 25.32°, 37.72°, 48.10°, 53.82°, 55.09°, 62.71°, 68.56°, 70.59°, and 75.03°. The observed peaks correspond to the crystallographic planes of anatase TiO_2, specifically the (101), (004), (200), (105), (211), (204), (116), (220), and (215) planes (Figure 4a). The obtained XRD patterns exhibit a tetragonal structure and were

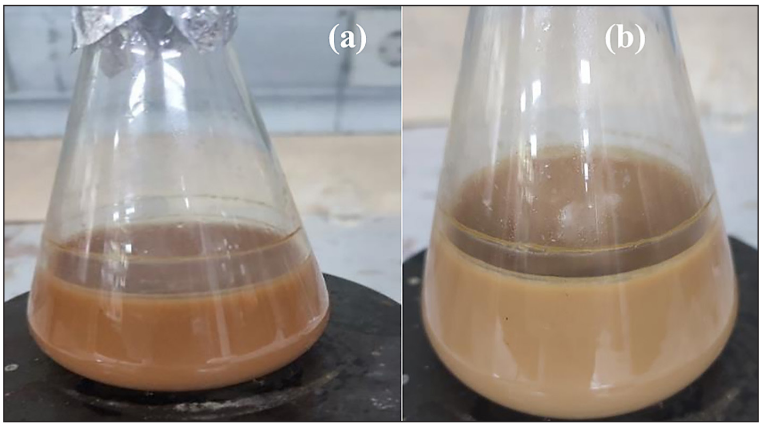

Figure 2. Observation of the (a) $TiCl_4$ solution with *Lansium domesticum,* (b) biosynthesized TiO_2 NPs

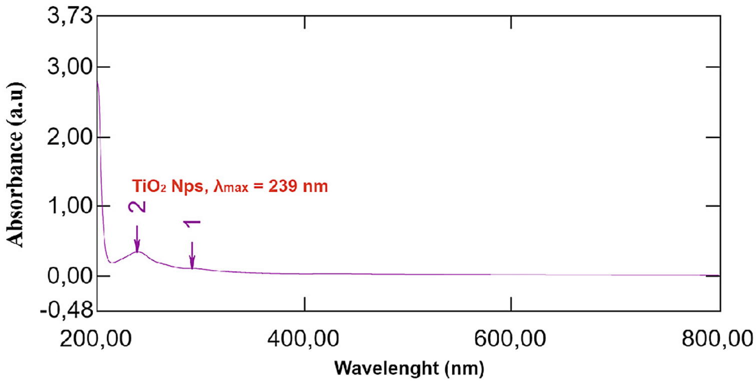

Figure 3. UV-vis spectrum of TiO_2 NPs synthesized using aqueous extracts of *Lansium domesticum*

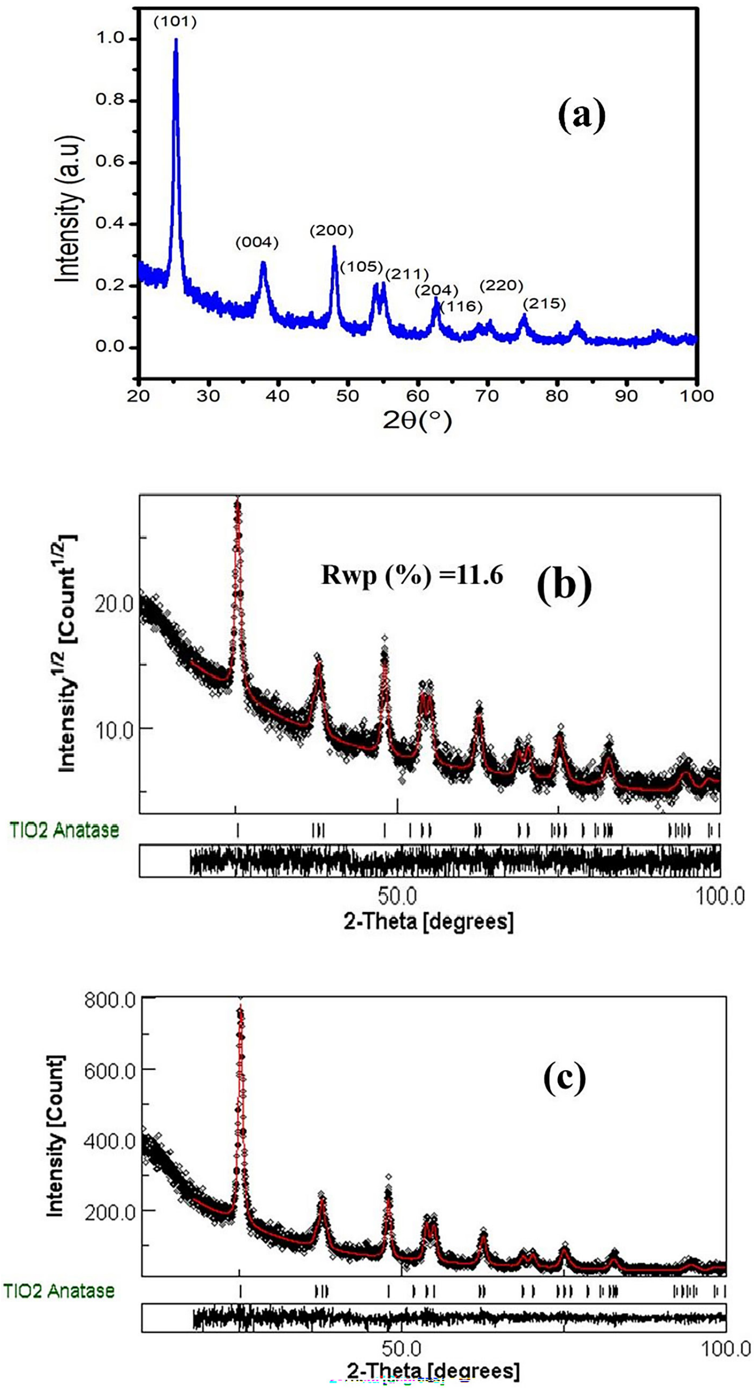

Figure 4. (a) XRD spectrum of TiO_2 NPs and (b–c) Rietveld analysis

compared to the standard JCPDS No. 21–1272 database. The physical characteristics of TiO_2 nanoparticles, including particle size and crystal structure, greatly influence their photocatalytic activity. Researchers expect the anatase crystal structure of TiO_2 to be used in the degradation of MO due to its larger surface area, lower recombination rate of holes and electron pairs compared to other phases, and stability at relatively lower temperatures compared to rutile and brookite (Mathew et al., 2021). Research on the synthesis of TiO_2 with the same method has been carried out previously by authors' team and published in the article Putri et al. (2019). The photocatalytic activity of TiO_2 NPs is influenced by several important factors, which can affect their effectiveness in the photocatalysis process, namely the size, shape, composition, material, concentration, and presence of TiO_2 NPs and others. On the basis of the results obtained, the synthesis of TiO_2 without extract shows an anatase crystal peak at 2θ value. However, calculations using the Scherrer formula show that the resulting TiO_2 crystal size, which is around 18 nm, and the photocatalytic activity are not as good as using TiO_2 NPs. Analysis of the TEM images also showed that the aggregation of the TiO_2 particles was less obvious (Putri et al., 2020), which indicates the linking between the aggregated particles is not as good as that found in the synthesis using extracts. In contrast, the research by Kim and Ehrman (2009) and Ohno et al. (2001) reported that the NPs obtained had an 80% anatase phase with a crystal size of 25 nm and a 20% rutile phase with a size of 85 nm. In addition, Viana et al. (2010) reported that the particle size of the TiO_2 NPs obtained was about 30 nm. A comparison of the synthesis performance of TiO_2 NPs was also described by Maurya et al. (2019) which showed that adding extracts significantly improved the performance of the material. In this study it was proven that photocatalytic activity indicated that TiO_2 NPs using *Lansium domesticum* extract peel exhibit markedly enhanced photocatalytic performance compared to commercially available anatase TiO_2 and TiO_2 NPs devoid of extract, as illustrated in Figure 9d. Furthermore, compared to conventional, green synthesis is likely to be more eco-friendly. On the basis of the X-ray diffraction (XRD) results, the average sizes of the catalyst crystallites were approximated using the Debye-Scherrer equation, as represented by:

$$D = k\,\lambda/(\beta \cos\theta) \tag{2}$$

where: D is the mean dimension of the crystal in nanometers, λ is the wavelength of the X-ray radiation which is 0.15418 nm, k is the Scherrer constant with a value of 0.9, θ is the diffraction angle and β is the full width at half maximum (FWHM) of the observed diffraction line.

The calculations indicate that the average size of the NPs crystallites is 43.8 nm. Reaction time has a significant effect on the reduction of TiO_2 NPs and plays a crucial role in determining the size of the final product (Shyam-Sundar et al., 2023). The diffraction patterns obtained were analyzed using the Rietveld method in MAUD (material analysis using diffraction (Figure 4b-c) software, Version 2.99. crystallographic information files (CIF) from the crystallography open database (COD) were used in the analysis, with the CIF selection based on references from sample analysis with XRD. These tests followed the methods outlined by Zein et al. (2022) and Heiba et al. (2022). A simulation esd performed to achieve the closest possible refinement. Additionally, in Figure 4b, Rietveld Refinement analysis employs two fundamental parameters, σ (Sigma values) and Rwp (R-weighted profile), to assess the congruence between empirical data and the derived model. The sigma (σ) value, quantified at 1.046% (falling within the conventional range of $1 < \sigma < 3$), signifies the degree of uncertainty or error associated with computed parameters, including atomic coordinates and lattice dimensions. Diminished σ values imply enhanced reliability and accuracy in these parameters.

The Rwp value, obtained as 11.6% (situated within the generally acceptable threshold of 10% < Rwp < 15%), serves as a weighted profile factor that is particularly responsive to discrepancies in high-intensity regions. This value offers an assessment of the overall quality of the model, where lower Rwp values denote a superior alignment between the model and the empirical data. While the potential for enhancement exists, these values indicate a relatively satisfactory correspondence between the model and the experimental observations. Hence, it is said that the level of fineness is suitable (Akhtar et al., 2019; Heiba et al., 2022).

FTIR analysis

Every molecule or chemical arrangement generates distinctive spectral patterns, rendering FTIR analysis a highly effective tool for chemical detection. The FTIR spectrum was used to determine the different functional groups present in the nanoparticles. Figure 5 shows the peel extract of *Lansium domesticum* prepared TiO_2 NPs FTIR spectra at different functional groups in each system. The peel extract of *Lansium domesticum* spectra revealed peaks at 1121 cm^{-1}, 1633 cm^{-1}, 2941 cm^{-1}, and 3326 cm^{-1}, signaling the existence of phytochemicals like triterpenoid, flavonoids, saponins, alkaloids, steroids, and phenolic compounds. Flavonoids stabilized and capped TiO_2 NPs. Due to their high OH group concentration, these phytochemicals were essential electron donors in metal reduction. The product spectra showed a peak at 834,654 cm^{-1} for Ti-O and Ti-O-Ti stretching vibrations and a peak at 1633 cm^{-1} for OH group bending vibrations before and

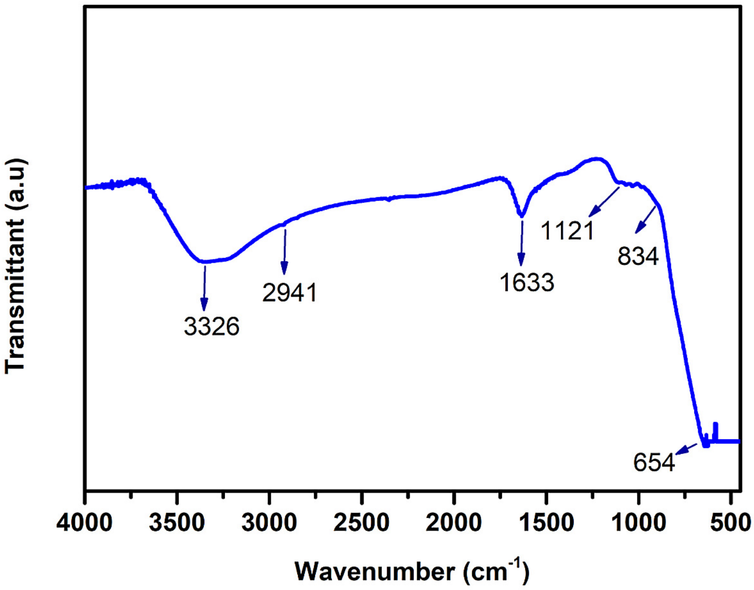

Figure 5. FT-IR spectral of aqueous extracts of TiO_2 NPs synthesized using *Lansium domesticum* peel extract

after calcination. The post-calcination presence of these radicals provides strong evidence that polyphenolic compounds were important both as bioreducing and capping agents in the production of TiO_2 NPs. The vibrational spectra of the TiO_2 NPs after calcination show that the calcination temperature of 500 °C ensures the elimination of certain phytochemical compounds. These compounds act as bioreducing or capping agents during the thermal process. Particle size and stability were controlled by the chemical interaction between the hydroxyl groups in the phenolic compounds and the surface of the TiO_2 NPs (Al Masoudi et al., 2023; Shimi et al., 2022). The suggested

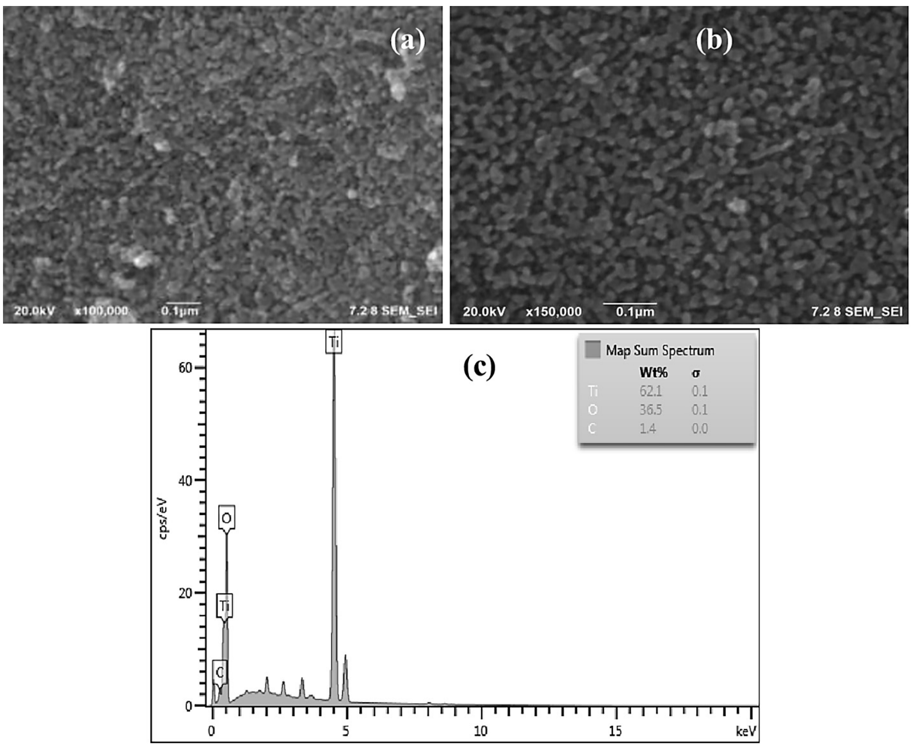

Figure 6. Structural and morphological analysis of TiO_2 NPs synthesized using extract peel of *Lansium domesticum* by (a) and (b) SEM analysis and determination of (c) EDX profil

mechanism entails capping TiO_2 nanoparticles with *Lansium domesticum* peel extract. In this process, polyphenol molecules such as ellagic acid, catechins, and quercetin interact with the TiO_2 Nps surface to control material transfer and the growth of the particles. This interaction also increases the thermodynamic stability of the NPs.

Field emission scanning electron microscopy (FE-SEM) analysis

In this study, a scanning electron microscopy analysis of evenly dispersed TiO_2 NPs on a surface that had both smooth and rough areas was conducted (Figure 6). The TiO_2 NPs exhibited a spherical morphology with a particle size of 80 nm. The produced TiO_2 NPs formed aggregates and had a spherical shape, with an average size ranging from 62 to 74 mm. The lack of direct contact between the NPs, even within the aggregates, suggests the stability of NPs (Binsabt et al., 2022; Kaur et al., 2019). It has been proposed that the observed aggregation might be due to an excess of H^+ ions from H_2O molecules present on the surface of the TiO_2 NPs. Figure 6 presents the FESEM images and EDX values of TiO_2 nanoparticles, showcasing their size, shape, and elemental composition. As illustrated in Figure 6c, the nanoparticles consisted of 62.1 wt% of titanium, 36.5% oxygen, and 14% carbon. The FESEM images reveal that the TiO_2 NPs are spherical and form aggregated structures with an average size of 17.6 nm. The particles appear to cluster together, creating a ball-like structure with a variety of small, medium, and large particles, leading to significant porosity. These spherical shapes are attributed to the influence of the peel extract *Lansium domesticum Correa* on the TiO_2 NP surfaces. The EDX analysis, shown in Figure 6c, identifies the presence of Ti and O, with Ti showing major peaks compared to O. The atomic and weight percentages confirm the presence of Ti and O in the TiO_2 NPs, highlighting the importance of O for radical formation.

These radicals are highly useful in biological and water remediation processes, demonstrating the successful reduction of $TiCl_4$ to form TiO_2. The use of *Lansium domesticum Correa* peels extracts as the bioreducing and capping agent produced the smallest TiO_2 NPs, which is supported by previous research using different plant peel extracts, as summarized in Table 2.

Table 2. The synthesized TiO_2 NPs from different peel extracts

Titanium precursor	Plant extract	Crystalline phase	Particle size (nm)	References
$TiCl_4$	*Lansium domesticum* peel	Anatase	17.6	This study
TTIP	Combine extract of *Allium sativum* and *Allium cepa L.* peel	Anatase	22	(Ali et al., 2023)
$Ti(NO_3)_4$	*Nephelium lappaceum L.* fruit peel	Anatase	70, 90	(Isacfranklin et al., 2021)
TTIP	*Solanum tuberosum* peel / potato peel	Combination of rutile and anatase structure	34–53	(Girigoswami et al., 2024)
TTIP	*Citrussinesis* peel	Anatase	75–85	(Oleiwi et al., 2024)
TTIP	*Juglans regia*	Anatase & rutile	19–23	(Heydari and Ghadam, 2023)
$Ti(OCH_2CH_2CH_2CH_3)_4$	*Cinnamon (C. zeylanicum bark)*	Anatase	70–150	(Nabi et al., 2020)
TTIP	*Garcinia mangostana*	Anatase & rutile	147	(Ahn et al., 2022)
TiO_2	*Prunus domestica L.* (Plum)	Anatase	47.1, 63.21	(Ajmal et al., 2019)
	Prunus persia L. (Peach)	Anatase	200	
	Actinidia deliciosa (Kiwi)	Anatase	54.17, 85.13	
$TiCl_4$	*Citrus sinensis*	Anatase	17–21	(Fall et al., 2019)
TTIP	*Punica granatum*	Anatase	92.8	(Abu-Dalo et al., 2019)
TiO_2 bulk powder	*Citrus limon*	Anatase	80–140	(Nabi et al., 2022)
$Ti(OCH_2CH_2CH_2CH_3)_4$	*Musa acuminata*	Anatase	22.4	(Olana et al., 2022)
$TiCl_3$	*Mangifera indica*	Anatase	18.1	(Isnaeni et al., 2021)

Particle size analyzer analysis

The average particle size was determined through the utilization of a Particle Size Analyzer, a sophisticated instrument widely employed in the field of nanotechnology for such measurements. The material under investigation was meticulously dispersed in distilled water with the aid of an ultra-sonicator, a high-tech device known for its ability to achieve complete dispersion of particles. It is crucial to note that the process of dispersing nanoparticles is a critical step in various scientific experiments and applications. a comprehensive understanding of the particle size distribution is required (Rao et al., 2016). The aforementioned analysis revealed an average particle size of 43.2 nm, a crucial metric in nanoscience and materials research (Figure 7). These findings were further corroborated by the XRD analysis, which provided insights into the average crystallite size of the material under study, thus enhancing the reliability and accuracy of the obtained results.

BET analysis

N2 adsorption-desorption isotherms were measured for TiO_2 NPs with a surface area and pore size analyzer. The surface area of the TiO_2 NPs was evaluated through BET analysis, while

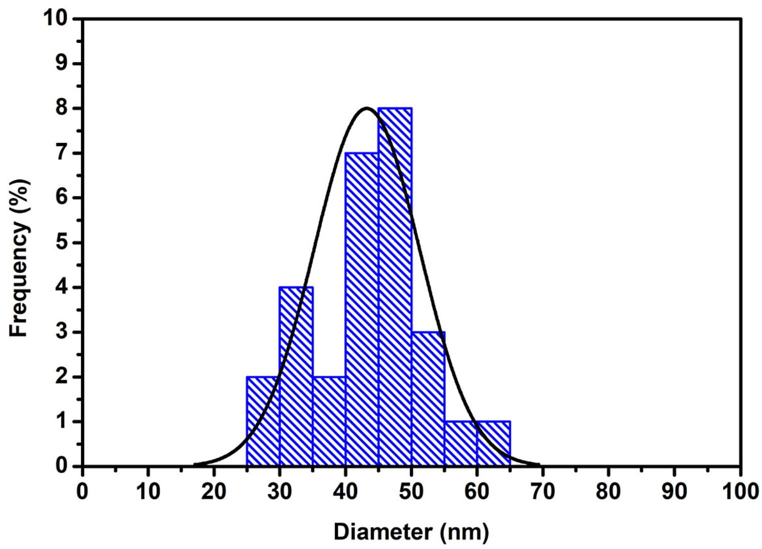

Figure 7. Particle size distribution of TiO_2 NPs

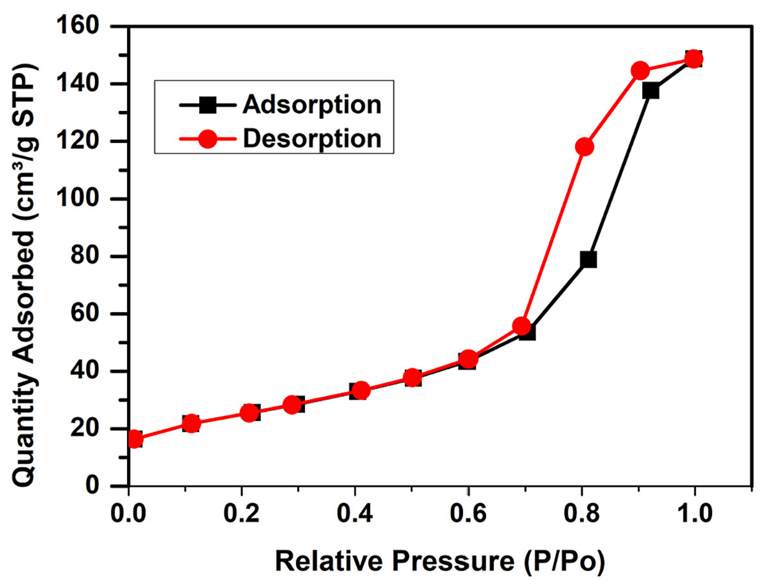

Figure 8. N2 Adsorption/desorption isotherm of the green synthesized TiO_2 NPs

pore volume and size distribution were determined with BJH analysis (Figure 8).

Brunauer-Emmett-Teller (BET) analysis uncovers a specific surface area of 88,0470 m²/g (50–200 m²/g), which aligns with an optimal range for photocatalytic action, as it signifies a greater number of available active sites for the photocatalytic reaction. Moreover, the average pore diameter of 15,2281 nm (2–50 nm) indicates an augmented potential for interaction between the material and MO pollutants, thereby facilitating enhanced photocatalytic activity. The total pore volume of 0.2299 cm³/g (0.1–0.5 cm³/g) is also advantageous, as a larger pore volume provides additional space for photocatalytic interactions. All these parameters reside within the preferred range and substantiate the effectiveness of the photocatalytic process (Goutam et al., 2018).

Photocatalytic activity

The degradation of the dye MO through photocatalysis was studied using synthesized TiO_2 NPs under different light sources, including solar light, visible light, UV-A, and UV-C, 6 mg L^{-1} MO was added to a variation of TiO_2 NPs (Figure 9a). It is evident from the analysis that UV-A rays exhibit optimal conditions when juxtaposed with the remaining three rays, primarily because UV-A and MO share wavelengths falling within the similar spectrum of 400–500 nm (464 nm), thus suggesting a significant correlation between the two entities (Gautam et al., 2023).

The photocatalytic activity of the synthesized TiO_2 NPs for degradation of MO dye was evaluated. The TiO_2 NPs demonstrated a photocatalytic efficiency of approximately 90%. The phase and particle size of the TiO_2 NPs likely played a role in this enhanced performance. These results indicate that using *Lansium domesticum* peel extract in the synthesis of TiO_2 produced pure anatase with small particle sizes, thereby improving its effectiveness in degrading MO dyes (Figure 9c), The difference can be seen without the addition of TiO_2 NPs (MO 6 mg L^{-1}, UV-A light) (Figure 9b).

The figure also demonstrated that increasing the TiO_2-NP dose enhanced MO degradation, indicating the production of more free radicals.

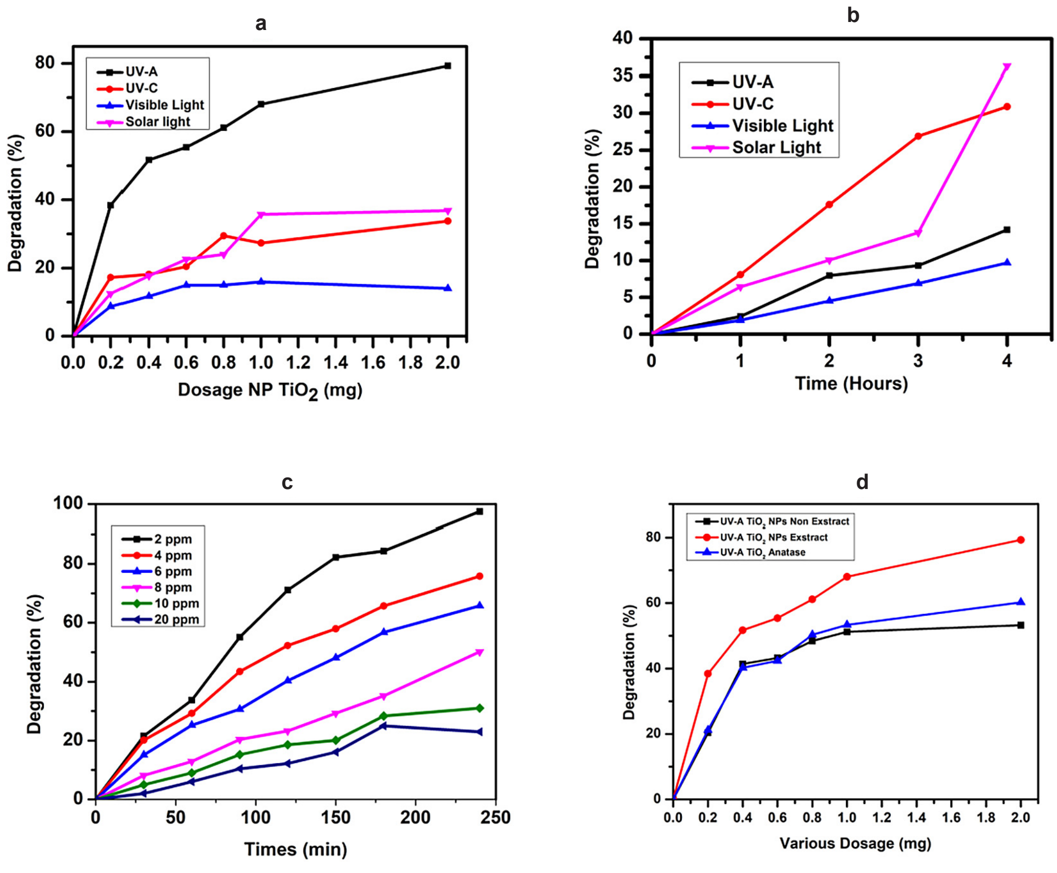

Figure 9. Impact of parameters on dye degradation: (a) catalyst dosage and light source, (b) absence of TiO_2 NPs and light source, (c) UV-A light and TiO_2 NPs, (d) photocatalytic activity comparison

With more active sites on the surface of the TiO_2 NPs, more photons were absorbed by the catalyst. This facilitated the photocatalytic reaction. Direct photolysis and adsorption were also carried out as a control. Under UV light, the electrons in the TiO_2 NPs are excited from the valence band to the conduction band, creating a hole (H+), an electron (E^-), and a hydroxyl radical (OH-), oxidizing the MO dye to a simpler compound, as shown in Figure 11 (Rehman et al., 2022). The study demonstrated that TiO_2 NPs containing *Lansium domesticum* extract peel significantly improve photocatalytic performance compared to the commercially available anatase TiO_2 and TiO_2 NPs without extract. As illustrated in Figure 9d, the TiO_2 NPs using extract attained a degradation efficiency of 79.31%. In contrast, their counterparts lacking extract registered a mere 53.23%, and the commercial anatase TiO_2 displayed a degradation efficiency of 60.22%. The natural extract of Lansium domesticum peel might improve the photocatalytic performance of TiO_2 nanoparticles. Phytochemicals in the extract, such as flavonoids and phenolics, alter the surface of the TiO_2 nanoparticles, thus increasing the absorption of both visible light and UV light. Besides, the extract reduces electron-hole recombination, prolonging the lifetime of charge carriers. It also improves surface properties, which results in smaller particle sizes, higher surface area, and improved dispersion. The extract also introduces new surface functional groups, thus improving the adsorption of organic pollutants. The presence of natural elements in the extract might further lead to the creation of some defect sites or narrowing of the bandgap of TiO_2.

The photocatalysis process degrades MO by attacking and breaking the azo bond (-N=N-), resulting in simpler and less toxic compounds (Rathi and Rejo, 2023; Safni et al., 2024). The mechanism of dye degradation is shown in Figure 10. The potency of TiO_2 NPs in disintegrating MO in aqueous environments is attributed to its formidable oxidizing capacity, remarkable stability, and minimal toxicity, along with its distinctive capability to produce reactive oxygen species (ROS) upon exposure to UV light.

The use of *Lansium domesticum* peel extract as a bioreducing and capping agent produces the smallest TiO_2 NPs (Table 2) and has good photocatalytic activity, supported by previous studies

Table 3. Photocatalytic activity of TiO_2 Nps using different plant extracts

Dye	Plant extract	Concentration of dye	Catalyst dosage	Exposure time	Percentage removal	Ref
RO-4 dye	Carica papaya leaves	-	15 mg, 20 mg, 25 mg and 30 mg	180 min at 3.5 pH	91.19%	(Harpreet Kaur et al., 2019)
Methylene blue	Justicia gendarussa leaves	200 mL	10 mg	75 min	-	(Senthilkumar & Rajendran, 2018)
Indigo carmine Bromothymol blue Rhodamine B	Achyranthes aspera leaf	25 ppm	0.20 mg	60 min	95% 94% 93%	(Ahmad et al., 2024)
Methylene blue		-	-	60 min	96%	
Acid Blue 113	*Tinospora cordifolia*	10–20 mg/L		80 min	94.43%	(Ravi Saini, 2023)
Methylene blue	Commelina benghanlensis	20 ppm	30 mg	120 min	65%	(Bopape et al., 2023)
Methyl orange	Azadirachta indica leaf	20 mg/L	0.1 g	270 min	98.62%	(Aouissi et al., 2022)
Methylene blue Methyl orange	Syringodium isoetifolium	-	60 μg/mL	120 min	83 % 58%	(Velmani Sundar et al., 2024)
Rhodamine b	Acorus calamus leaf			120 min	96,59%	(Ansari et al., 2022)
Methylene blue	Syzygium cumini leaves	10 ppm	100 mg	120 min	86,60%	(Khan et al., 2024)
Methyl orange	Peel extract of Parkia speciosa	3 ppm	1 mg L^{-1}	240 min 3 pH	97.79%	(Khoiriah & Putri, 2024)
Methylene blue	Mulberry plant	10 ppm	10 mg	120 min	120%	(Shimi, Ahmed et al., 2022)
Methyl orange	*Lansium domesticum*	2 ppm	0.0010 g	240 min	97.50%	This study

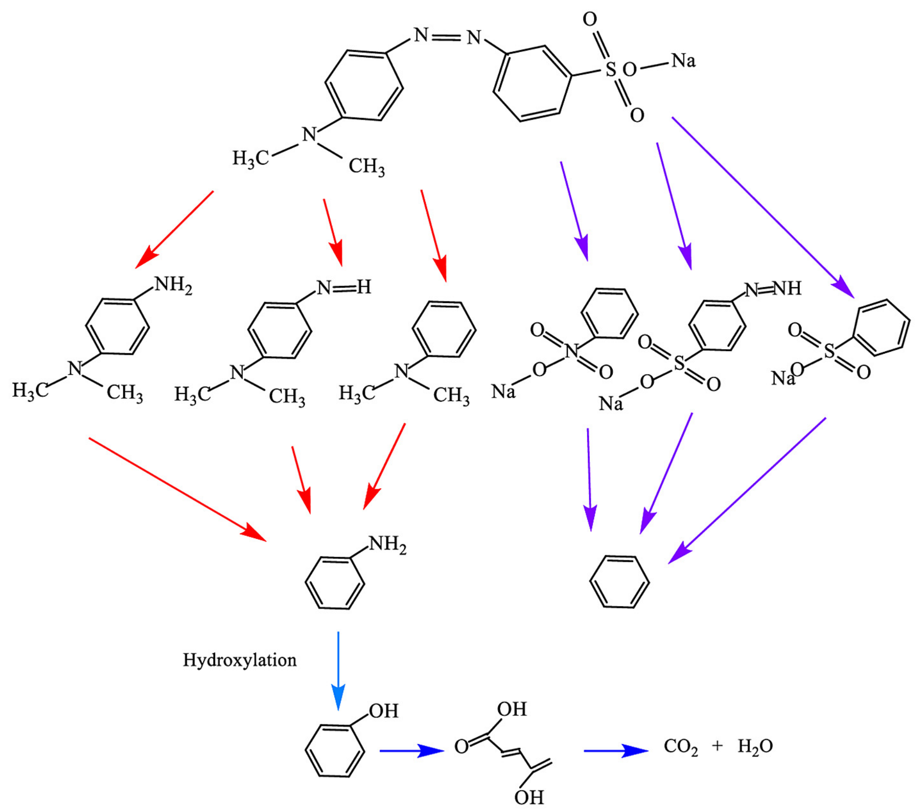

Figure 10. Schematic diagram of the photocatalytic degradation mechanism of MO dye

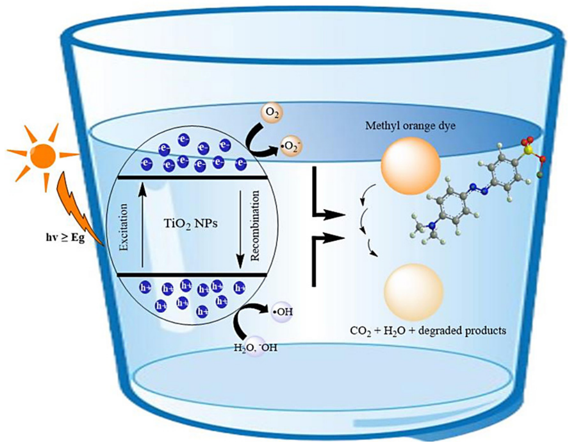

Figure 11. Mechanism of photocatalytic degradation using green synthesized TiO_2 NPs

using different plant bark extracts, which can be seen from the percentage removal, exposure time, dosage catalyst and concentration of dye from several dyes as summarized in Table 3. The proposed photocatalytic degradation pathway scheme focuses on the transformation of intermediate species, which precedes aromatic ring-opening. It begins with MO demethylation and hydroxylation, which involve the homolytic rupture of the nitrogen-carbon bond, leading to the substitution of a methyl group with a hydrogen atom. This process is likely to result in products formed by multiple substitutions of hydroxyl groups (Figure 10). The by-products of MO degradation are determined by individual demethylation and hydroxylation processes and their combinations.

The scavengers study

The study identified reactive species FC (h+), IPA (•OH), BQ (O_2•⁻), and $K_2Cr_2O_7$ for electrons as the most influential radical species during the photocatalytic reaction over TiO_2 NPs 1.0 mg L^{-1}. The addition of scavenger species decreases photocatalytic activity, as the scavenger solution captures radical species. The effect of scavengers on MO degradation was evaluated to understand the pathway degradation and confirm the main contribution of reactive species. The degradation efficiencies were 80.53% (UV A) and 19.53% (UV-VIS) after 180 minutes of photocatalysis (Table 4) (Figure 12). Electro-hole pairs on the TiO_2 surface are produced by adsorbing UV photons. The remaining methyl orange concentration decreases with IPA, FC, and BQ additions. O_2•⁻ is the primary reactive species contributing

Table 4. The removal efficiency of MO in the presence of various scavengers involved in the radical and reaction mechanisms

Scavengers	Involved radicals	Degradation after 180 minutes (%)		Reaction mechanism
		UV A	UV-Vis	
Without scavengers	-	80.53	19.53	-
Formic acid 20 mM	h^+	55.4	30.02	$HCOO- + h + \rightarrow CO_2 + H+$
Isopropyl-alcohol 10 mL	HO	61.17	16.23	$HO\cdot + (CH_3)_2CH - OH \rightarrow H_2O + (CH_3)C \cdot - OH$
$K_2Cr_2O_7$ 1 mM	e^-	22.30	25.45	$Cr_2O^{2-}{}_7 + 14H^+ + 6e^- \rightarrow 2Cr^{3+} + 7H_2O$
0.001 g benzoquinone	$O_2^{\cdot-}$	32.33	12.12	$BQ + O_2^{\cdot-} \rightarrow BQ\cdot- + O_2$

Note: Experimental condition: MO initial concentration = 6 mg/L, photocatalyst: TiO_2 NPs with a concentration of 0.1 mg/L.

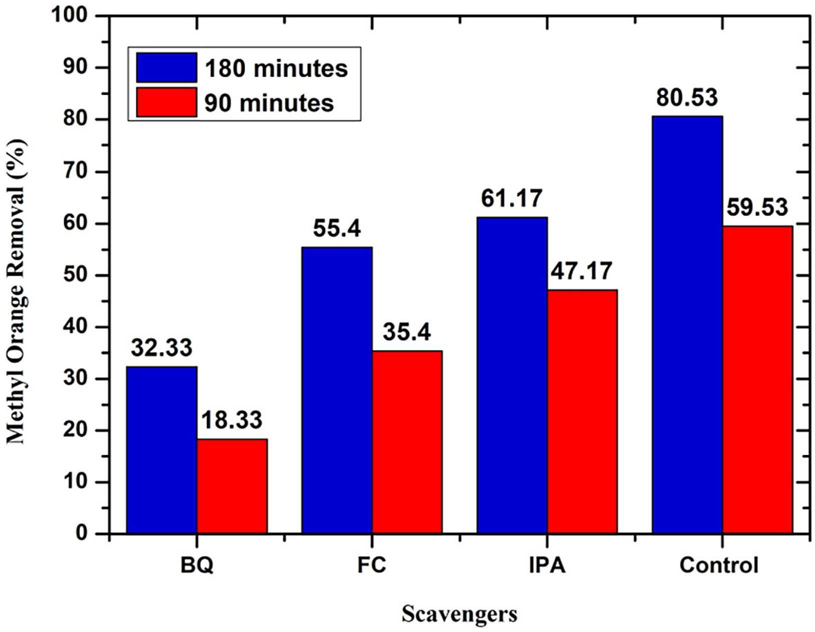

Figure 12. The impact of scavengers on the photocatalytic performance of TiO_2 nanoparticles at a concentration of 0.1 mg L^{-1} and methyl orange (MO) at 6 mg L^{-1}

to photocatalytic activity. FC, as a scavenger, plays a secondary role. The band gap energy of prepared TiO_2 is similar, suggesting impurities influence electron-hole separation, enhancing the reaction rate of MO oxidation.

CONCLUSIONS

TiO_2 NPs have been successfully synthesized using the peel extract of *Lansium domesticum* Correa as a bioreducing and capping agent. The phytochemical characteristics of the TiO_2 NPs that were synthesized using UV-Vis spectrophotometry, FTIR, XRD, FESEM, PSA, and BET. The characterization results showed that the synthesized TiO_2 was pure crystalline in the anatase phase, stable, and spherical with a size of 17.6 nm. Phytochemical screening and FTIR analysis revealed that compounds like alkaloids, saponins, flavonoids, triterpenoids, and steroids functioned as effective and eco-friendly bioreducing and capping agents. They have synthesized TiO_2 degraded 97.74% MO dye within 240 minutes. This study demonstrated that the biosynthesized TiO_2 NP showed enhanced photocatalytic activity. Researchers are motivated by these positive findings to investigate natural alternatives and create advanced, more secure techniques for producing metal oxide nanomaterials. The findings represent an important technological opportunity for the development of TiO_2-based nanotechnological materials in the light of customer needs and industrial conditions.

Acknowledgments

This research was financially supported by the Organization Research and Innovation Agency, National Research and Innovation Agency of Indonesia through "Degree by Research". The authors also thank Andalas University for providing supporting facilities during our research.

REFERENCES

1. Abdallah, H. M., Mohamed, G. A., Ibrahim, S. R. M. (2022). Lansium domesticum – A fruit with multi-benefits: traditional uses, phytochemicals, nutritional value, and bioactivities. *Nutrients*, *14*(7), 1–42. https://doi.org/10.3390/nu14071531
2. Abisharani, J. M., Devikala, S., Kumar, R. D., Arthnareeswari, M., Kamaraj, P. (2019). Green synthesis of TiO_2 nanoparticles using Cucurbita pepo seeds extract. *Materials Today: Proceedings*, *14*, 302–307.
3. Abu-Dalo, M., Jaradat, A., Albiss, B. A., Al-Rawashdeh, N, A.F. (2019). Green synthesis of TiO_2 NPs/pristine pomegranate peel extract nanocomposite and its antimicrobial activity for water disinfection. *Journal of Environmental Chemical Engineering*, *7*, 103370 Contents.
4. Ahmad, W., Kumar, S., Ahmed, S. (2024). Microwave-assisted one-step biosynthesis of titanium dioxide nanoparticles: Antibacterial, antioxidant, and photocatalytic properties. *Kuwait Journal of Science*, *51*(2), 100203. https://doi.org/10.1016/j.kjs.2024.100203
5. Ahmad, W., Singh, A., Jaiswal, K. K., Gupta, P. (2021). Green synthesis of photocatalytic tio_2 nanoparticles for potential application in photochemical degradation of ornidazole. *Journal of Inorganic and Organometallic Polymers and Materials*, *31*(2), 614–623. https://doi.org/10.1007/s10904-020-01703-6
6. Ahn, E.-Y., Shin, S.-W., Kim, K., Park, Y. (2022). Facile green synthesis of titanium dioxide nanoparticles by upcycling mangosteen (*Garcinia mangostana*) pericarp extract. *Nanoscale research letters* 17(1), 40. https://doi.org/10.1186/s11671-022-03678-4
7. Ajmal, N., Saraswat, K., Bakht, M. A., Riadi, Y., Ahsan, M. J., Noushad, M. (2019). Cost-effective and eco-friendly synthesis of titanium dioxide (TiO_2) nanoparticles using fruit's peel agro-waste extracts: characterization, in vitro antibacterial, antioxidant activities. *Green Chemistry Letters and Reviews*, *12*(3), 244–254. https://doi.org/10.1080/17518253.2019.1629641
8. Akhtar, M. N., Babar, M., Qamar, S., Rehman, Z. ur, Khan, M. A. (2019). Structural Rietveld refinement and magnetic features of prosademium (Pr) doped Cu nanocrystalline spinel ferrites. *Ceramics International*, *45*(8), 10187–10195. https://doi.org/10.1016/j.ceramint.2019.02.069
9. Akritidis, J. (2022). Biosynthesis of TiO_2 nanoparticles and their application as catalyst in biodiesel production. *Clean Energy Production Technologies*. https://doi.org/https://doi.org/10.1007/978-981-16-9356-4_6
10. Al Masoudi, L. M., Alqurashi, A. S., Abu Zaid, A., Hamdi, H. (2023). Characterization and biological studies of synthesized titanium dioxide nanoparticles from leaf extract of *Juniperus phoenicea* (L.) Growing in Taif Region, Saudi Arabia. *Processes*, *11*(1), 1–15. https://doi.org/10.3390/pr1101027
11. Ali, H., Dixit, S., Almutairi, B. O., Yadav, N. (2023). Synthesis and characterization of eco-friendly TiO_2 nanoparticle from combine extract of onion and garlic peel. *Journal of King Saud University - Science*, *35*(8), 102918. https://doi.org/10.1016/j.jksus.2023.10291
12. Ansari, A., Siddiqui, V. U., Rehman, W. U., Akram, M. K., Siddiqi, W. A., Alosaimi, A. M., Hussein, M. A., Rafatullah, M. (2022). Correction: green synthesis of TiO_2 nanoparticles using acorus calamus leaf extract and evaluating its photocatalytic and in vitro antimicrobial activity *Catalysts, 12*(181), 10.3390/catal12020181. *Catalysts*, *12*(11). https://doi.org/10.3390/catal12111451
13. Aouissi, I. E., Chandren, S., Basar, N., Wan Ibrahim, W. N. (2022). Phytochemical-assisted synthesis of titania nanoparticles using azadirachta indica leaf extract as photocatalyst in the photodegradation of methyl orange. *Bulletin of Chemical Reaction Engineering and Catalysis*, *17*(4), 683–698. https://doi.org/10.9767/bcrec.17.4.15581.683-698
14. Aravind, M., Amalanathan, M., Aslam, S., Noor, A. E., Jini, D., Majeed, S., Velusamy, P., Alothman, A. A., Alshgari, R. A., Mushab, M. S. S., Sillanpaa, M. (2023). Hydrothermally synthesized Ag-TiO_2 nanofibers (NFs) for photocatalytic dye degradation and antibacterial activity. *Chemosphere 321*, 138077. https://doi.org/10.1016/j.chemosphere.2023.138077
15. Balaraman, P., Balasubramanian, B., Liu, W. Kaliannan, D., Durai, M., Kamyab, H., Alwetaishi, M., Maluventhen, V., Ashokkumar, V., Chelliapan, S., Maruthupandian, A. (2022). Sargassum myriocystum-mediated TiO_2-nanoparticles and their antimicrobial, larvicidal activities and enhanced photocatalytic degradation of various dyes. *Environmental Research*, *204*, 112278.
16. Binsabt, M., Sagar, V., Singh, J., Rawat, M., Shaban, M. (2022). Green synthesis of CS-TiO2 NPs for efficient photocatalytic degradation of methylene blue dye. *Polymers*, *14*(13), 1–12. https://doi.org/10.3390/polym14132677
17. Bopape, D. A., Tetana, Z. N., Mabuba, N., Motaung,

D. E., Hintsho-Mbita, N. C. (2023). Biosynthesis of TiO_2 nanoparticles using Commelina benghanlensis for the photodegradation of methylene blue dye and antibiotics: Effect of plant concentration. *Results in Chemistry*, *5*, 100825. https://doi.org/10.1016/j.rechem.2023.100825

18. Bößl, F., Comyn, T. P., Cowin, P. I., García-García, F. R., Tudela, I. (2021). Piezocatalytic degradation of pollutants in water: Importance of catalyst size, poling and excitation mode. *Chemical Engineering Journal Advances*, *7*(May), 100133. https://doi.org/10.1016/j.ceja.2021.100133
19. Buazar, F., Bavi, M., Kroushawi, F., Halvani, M., Khaledi-Nasab, A., Hossieni, S. A. (2016). Potato extract as reducing agent and stabiliser in a facile green one-step synthesis of ZnO nanoparticles. *Journal of Experimental Nanoscience*, *11*(3), 175–184. https://doi.org/10.1080/17458080.2015.1039610
20. Dalal, C., Garg, A. K., Jain, N., Naziruddin, A. R., Prajapati, R. K., Choudhary, S. K., Sonkar, S. K. (2023). Sunlight-assisted photocatalytic degradation of azo-dye using zinc-sulfide embedded reduced graphene oxide. *Solar Energy*, *251*, 315–324. https://doi.org/10.1016/j.solener.2023.01.017
21. Deliza, Safni, R. et al. (2014). Degradasi Rhodamin B secara fotokatalisis dan ozonolisis dengan penambahan TiO_2-$NiFe_2O_4$, TiO_2-$CuFe_2O_4$, dan TiO_2-$MnFe_2O_4$. *Jurnal Riset Kimia*, *7*.
22. Devikala, S., Abisharani, J. M., Bharath, M. (2021). Biosynthesis of TiO_2 nanoparticles from Caesalpinia pulcherrima flower extracts. *Materials Today: Proceedings*, *40*, S185–S188.
23. Fall, A., Ngom, I., Bakayoko, M., Sylla, N. F., Mohamed, H. E. A., Jadvi, K., Kaviyarasu, K., Ngom, B. D. (2019). Biosynthesis of TiO_2 nanoparticles by using natural extract of Citrus sinensis. *Materials Today: Proceedings*, *36*, 349–356. https://doi.org/10.1016/j.matpr.2020.04.13
24. Gautam, I., Grady, T., Fernando, H. (2023). Degradation of the dye methyl orange using cow and goat milk iron nanoparticles. *Green Chemistry Letters and Reviews*, *16*(1), 2174818. https://doi.org/10.1080/17518253.2023.2174818
25. Girigoswami, A., Deepika, B., Pandurangan, A. K., Girigoswami, K. (2024). Preparation of titanium dioxide nanoparticles from Solanum Tuberosum peel extract and its applications. *Artificial Cells, Nanomedicine and Biotechnology*, *52*(1), 59–68. https://doi.org/10.1080/21691401.2023.2301068
26. Goutam, S. P., Saxena, G., Singh, V., Yadav, A. K., Bharagava, R. N., Thapa, K. B. (2018). Green synthesis of TiO_2 nanoparticles using leaf extract of *Jatropha curcas* L. for photocatalytic degradation of tannery wastewater. *Chemical Engineering Journal*, *336*(December 2017), 386–396. https://doi.org/10.1016/j.cej.2017.12.029
27. Kaur, H., Kaur, S., Singh, J., Rawat, M. S. K. (2019). Expanding horizon: green synthesis of TiO_2 nanoparticles using Carica papaya leaves for photocatalysis application. *Materials Research Express*, *6*, 095034.
28. Heiba, Z. K., Mohamed, M. B., Badawi, A. (2022). Structural and optical characteristic of Cu-doped TiO_2 thin film. *Journal of Inorganic and Organometallic Polymers and Materials*, *32*(8), 2853–2862. https://doi.org/10.1007/s10904-022-02312-1
29. Heiba, Z. K., Mohamed, M. B., Badawi, A., Abdellatief, M. (2022). Effect of vanadium and tungsten doping on the structural, optical, and electronic characteristics of TiO_2 nanoparticles. *Journal of Materials Science: Materials in Electronics*, *33*(13), 10399–10409. https://doi.org/10.1007/s10854-022-08027-w
30. Heydari, Z., Ghadam, P. (2023). Biosynthesis of titanium dioxide nanoparticles by the aqueous extract of Juglans regia green husk. *Materials Proceedings*, *14*, 1–8. https://doi.org/10.3390/iocn2023-14482
31. Ilyasu, N. S., Adams, N. H., Umar, R., Ishaya, S., Nweke, O. D., Usman, S., Jagaba, A. H., Yakasai, H. M. (2024). Palm oil mill effluent degradation by a novel strain of Bacillus sp. isolated from contaminated environment. *Case Studies in Chemical and Environmental Engineering*, *9*(January), 100637. https://doi.org/10.1016/j.cscee.2024.100637
32. Isacfranklin, M., Yuvakkumar, R., Ravi, G., Kumar, P., Saravanakumar, B., Velauthapillai, D., Alahmadi, T. A., Alharbi, S. A. (2021). Biomedical application of single anatase phase TiO_2 nanoparticles with addition of Rambutan (*Nephelium lappaceum* L.) fruit peel extract. *Applied Nanoscience (Switzerland)*, *11*(2), 699–708. https://doi.org/10.1007/s13204-020-01599-1
33. Isnaeni, I. N., Sumiarsa, D., Primadona, I. (2021). Green synthesis of different TiO_2 nanoparticle phases using mango-peel extract. In *Materials Letters*. Elsevier.
34. Jalill, R. D. H. A., Nuaman, R. S., Abd, A. N. (2016). Biological synthesis of Titanium Dioxide nanoparticles by *Curcuma longa* plant extract and study its biological properties. *World Scientific News*, *49*(2), 204–222.
35. Chanani, J., Foad Buazar, Y. N. (2023). Promoted photocatalytic activity of green titanium oxide-clay nanocomposite toward polychlorinated biphenyl degradation in actual samples. *Water, Air, & Soil Pollution*, *234*(364).
36. Kaur, H., Kaur, S., Singh, J., Rawat, Kumar, S. (2019). Expanding horizon: green synthesis of TiO_2 nanoparticles using *Carica papaya* leaves for photocatalysis application. *Materials Research,* https://doi.org/10.1088/2053-1591/ab2ec5.
37. Kaur, H., Kaur, S., Singh, J., Rawat, M., Kumar, S. (2019). Expanding horizon: Green synthesis of TiO_2

nanoparticles using *Carica papaya* leaves for photocatalysis application. *Materials Research Express*, *6*(9). https://doi.org/10.1088/2053-1591/ab2ec5

38. Khalafi, T., Buazar, F., Ghanemi, K. (2019). Phycosynthesis and enhanced photocatalytic activity of zinc oxide nanoparticles toward organosulfur pollutants. *Scientific Reports*, *9*(1), 1–10. https://doi.org/10.1038/s41598-019-43368-3
39. Khaleel, A. H., Rafi, S. M., Merajuddin, K., Alkhathlan H. Z., Farooq, A. S., Mufsir, K., Assal Mohamed E., Al-Warthan A., Rafiq H. S. M., Nawaz T. M., Tabrez, S., Mousa, A. A. and M. K. (2022). Pulicaria undulata extract-mediated eco-friendly preparation of TiO_2 nanoparticles for photocatalytic degradation of methylene blue and methyl orange. *ACS Publications*, *7*, 4812–4820. https://doi.org/10.1021/acsomega.1c05090
40. Khan, A., Raza, A., Hashem, A., Dolores Avila-Quezada, G., Fathi Abd_Allah, E., Ahmad, F., Ahmad, A. (2024). Green fabrication of titanium dioxide nanoparticles via Syzygium cumini leaves extract: characterizations, photocatalytic activity and nematicidal evaluation. *Green Chemistry Letters and Reviews*, *17*(1). https://doi.org/10.1080/17518253.2024.2331063
41. Khoiriah, K., Putri, R. A. (2024). Biosynthesis of titanium dioxide nanoparticles using peel extract of Parkia speciosa for methyl orange degradation. *South African Journal of Botany*, *170*, 120–129. https://doi.org/10.1016/j.sajb.2024.05.021
42. Kim, S., Ehrman, S. H. (2009). Photocatalytic activity of a surface-modified anatase and rutile titania nanoparticle mixture. *Journal of Colloid and Interface Science*, *338*(1), 304–307. https://doi.org/10.1016/j.jcis.2009.06.047
43. Koopi, H., Buazar, F. (2018). A novel one-pot biosynthesis of pure alpha aluminum oxide nanoparticles using the macroalgae Sargassum ilicifolium: A green marine approach. *Ceramics International*, *44*(8), 8940–8945. https://doi.org/10.1016/j.ceramint.2018.02.091
44. Souheila, L., Meneceur, S., Bouafia, A., Laouini, S. E., Alshareef, S. A., Al-Essa, K., Almukhlifi, H. A. (2024). Biofabrication of NiO and NiO-decorated Fe nanocomposite efficiency for removal of methylene blue from aqueous solution. *Biomass Conversion and Biorefinery*, *14*, 18469–18479. https://doi.org/https://doi.org/10.1007/s13399-023-03912-8
45. Li, W., Li, D., Wang, J., Shao, Y., You, J., Teng, F. (2013). Exploration of the active species in the photocatalytic degradation of methyl orange under UV light irradiation. *Journal of Molecular Catalysis A: Chemical*, *380*, 10–17. https://doi.org/10.1016/j.molcata.2013.09.001
46. Mathew, S. S., Sunny, N. E., Shanmugam, V. (2021). Green synthesis of anatase titanium dioxide nanoparticles using Cuminum cyminum seed extract; effect on Mung bean (*Vigna radiata*) seed germination. *Inorganic Chemistry Communications*, *126*(January), 108485. https://doi.org/10.1016/j.inoche.2021.108485
47. Maurya, I. C., Singh, S., Senapati, S., Srivastava, P., Bahadur, L. (2019). Green synthesis of TiO_2 nanoparticles using Bixa orellana seed extract and its application for solar cells. *Solar Energy*, *194*(October), 952–958. https://doi.org/10.1016/j.solener.2019.10.090
48. Nabi, G., Ain, Q. U., Tahir, M. B., Nadeem Riaz, K., Iqbal, T., Rafique, M., Hussain, S., Raza, W., Aslam, I., Rizwan, M. (2022). Green synthesis of TiO_2 nanoparticles using lemon peel extract: their optical and photocatalytic properties. *International Journal of Environmental Analytical Chemistry*, *102*(2), 434–442. https://doi.org/10.1080/03067319.2020.1722816
49. Nabi, G., Raza, W., Tahir, M. B. (2020). Green synthesis of TiO_2 nanoparticle using cinnamon powder extract and the study of optical properties. *Journal of Inorganic and Organometallic Polymers and Materials*, *30*(4), 1425–1429. https://doi.org/10.1007/s10904-019-01248-3
50. Ohno, T., Sarukawa, K., Tokieda, K., Matsumura, M. (2001). Morphology of a TiO_2 photocatalyst (Degussa, P-25) consisting of anatase and rutile crystalline phases. *Journal of Catalysis*, *203*(1), 82–86. https://doi.org/10.1006/jcat.2001.3316
51. Olana, M. H., Sabir, F. K., Bekele, E. T., Gonfa, B. A. (2022). Citrus sinensis and Musa acuminata peel waste extract mediated synthesis of TiO_2/rGO nanocomposites for photocatalytic degradation of methylene blue under visible light irradiation. *Bioinorganic Chemistry and Applications*, 1–21. https://doi.org/10.1155/2022/5978707
52. Oleiwi, H. F., Rahma, A. J., Salih, S. I., Beddai, A. A. (2024). Comparative study of sol-gel and green synthesis technique using orange peel extract to prepare TiO_2 Nanoparticles. *Baghdad Science Journal*, *21*(5), 1702. https://doi.org/10.21123/bsj.2023.8089
53. Patidar, V., Jain, P. (2017). Green synthesis of TiO_2 nanoparticle using moringa oleifera leaf extract. *International Research Journal of Engineering and Technology*, 470–474. www.irjet.net
54. Rajaram, P., Ambrose Rejo Jeice, K. J. (2023). Review of green synthesized TiO_2 nanoparticles for diverse applications. *Surfaces and Interfaces*, *39*(102912).
55. Rajaram, P., Ambrose Rejo Jeice, K. J. (2024). Influences of calcination temperature on titanium dioxide nanoparticles synthesized using Averrhoa carambola leaf extract: in vitro antimicrobial activity and UV-light catalyzed degradation of textile wastewater. *Biomass Conversion and Biorefinery*,

14, 20665–20678.

56. Putri, R. A., Safni, S., Jamarun, N., Septiani, U. (2019). Kinetics study and degradation pathway of methyl orange photodegradation in the presence of C-N-codoped TiO_2 catalyst. *Egyptian Journal of Chemistry*, *63*(Part 2), 563–575. https://doi.org/10.21608/ejchem.2019.14543.1883
57. Putri, R. A., Safni, S., Jamarun, N., Septiani, U., Kim, M. K., Zoh, K. D. (2020). Degradation and mineralization of violet-3B dye using C-N-codoped TiO_2 photocatalyst. *Environmental Engineering Research*, *25*(4), 529–535. https://doi.org/10.4491/eer.2019.196
58. Putri, R. A., Tursiloadi, S., Nurrahmah, E. F., Liandi, A. R., Arutanti, O. (2023). Synthesis of TiO_2-based photocatalyst from indonesia ilmenite ore for photodegradation of eriochrome black-t dye. *Water, Air, and Soil Pollution*, *234*(8). https://doi.org/10.1007/s11270-023-06584-2
59. Rahimi, S., Buazar, F., Larki, A. (2023). Efficient absorption and sensing of haloacetonitriles on fullerene C20 surface at DFT level. *Water, Air, and Soil Pollution*, *234*(7), 1–14. https://doi.org/10.1007/s11270-023-06447-w
60. Rao, K. G., Rao, K. V., Rajendar, V., Ashok, C., Chakra, C. S. (2016). *Green Synthesis of TiO 2 Nanoparticles Using Hibiscus Flower Extract*. *2*, 28–34.
61. Rathi, V. H., Rejo, A. (2023). Green fabrication of titanium dioxide nanoparticles and their applications in photocatalytic dye degradation and microbial activities. *Chemical Physics Impact*, *6*(March), 100197. https://doi.org/10.1016/j.chphi.2023.100197
62. Ravi Saini, P. K. (2023). Green synthesis of TiO_2 nanoparticles using Tinospora cordifolia plant extract & its potential application for photocatalysis and antibacterial activity. *Inorganic Chemistry Communications*, *156*, 111221.
63. Roopan, S. M. (2012). Efficient phyto-synthesis and structural characterization of rutile TiO_2 nanoparticles using Annona squamosa peel extract. *Spectrochimica Acta - Part A: Molecular and Biomolecular Spectroscopy*, *98*, 86–90. https://doi.org/10.1016/j.saa.2012.08.055
64. Safni, R. Z., Putri, R. A. D. (2024). Advancement in green synthesis of titanium dioxide : photocatalytic and larvicidal activities – A review. *Hydrogen*, *12*(February), 115–126.
65. Safni, Anggraini, D., Wellia, D. V., Khoiriah. (2015). Degradasi zat warna direct red-23 dan direct violet dengan metode ozonolisis, fotolisis dengan sinar UV dan cahaya matahari menggunakan katalis N-doped TiO_2. *Jurnal Litbang Industri*, *5*(2), 123–130.
66. Safni, S., Deliza, Anggraini, D., Dewi, R. S., Ulia, H., Wellia, D. V. (2016). Degradation of direct red-81 and direct yellow-27 by photolysis with UV-light and solar irradiation using C-N-codoped TiO_2. *Der Pharma Chemica*, *8*(12), 30–35.
67. Safni, Wellia, D. V., Komala, P. S., Putri, R. A. (2015). Degradation of yellow-GCN by photolysis with UV-light and solar irradiation using C-N-codoped TiO_2 catalyst. *Journal of Chemical and Pharmaceutical Research*, *7*(11), 306–311.
68. Sankar, R. (2015). Ultra-rapid photocatalytic activity of Azadirachta indica engineered colloidal titanium dioxide nanoparticles. *Applied Nanoscience (Switzerland)*, *5*(6), 731–736. https://doi.org/10.1007/s13204-014-0369-3
69. Senthilkumar, S., Rajendran, A. (2018). Biosynthesis of TiO_2 nanoparticles using Justicia gendarussa leaves for photocatalytic and toxicity studies. *Research on Chemical Intermediates*, *44*(10), 5923–5940. https://doi.org/10.1007/s11164-018-3464-3
70. Sepahvand, M., Buazar, F., Sayahi, M. H. (2020). Novel marine-based gold nanocatalyst in solvent-free synthesis of polyhydroquinoline derivatives: Green and sustainable protocol. *Applied Organometallic Chemistry*, *34*(12), 1–11. https://doi.org/10.1002/aoc.6000
71. Shimi, A. K., Ahmed, H. M., Wahab, M., Katheria, S., Wabaidur, S. M., Eldesoky, G. E., Islam, M. A., Rane, K. P. (2022). Synthesis and applications of green synthesized TiO_2 nanoparticles for photocatalytic dye degradation and antibacterial activity. *Journal of Nanomaterials*, *2022*. https://doi.org/10.1155/2022/7060388
72. Shimi, A. K., Wabaidur, S. M., Siddiqui, M. R., Islam, M. A., Rane, K. P., Jeevan, T. S. A. (2022). Photocatalytic activity of green construction TiO_2 nanoparticles from Phyllanthus niruri leaf extract. *Journal of Nanomaterials*, 1–11. https://doi.org/10.1155/2022/7011539
73. Shyam-Sundar, N., Karthi, S., Senthil-Nathan, S., Narayanan, K. R., Santoshkumar, B., Sivanesh, H., Chanthini, K. M. P., Stanley-Raja, V., Ramasubramanian, R., Abdel-Megeed, A., Malafaia, G. (2023). Eco-friendly biosynthesis of TiO_2 nanoparticles using Desmostachya bipinnata extract: Larvicidal and pupicidal potential against Aedes aegypti and Spodoptera litura and acute toxicity in non-target organisms. *Science of the Total Environment*, *858*(October 2022), 159512. https://doi.org/10.1016/j.scitotenv.2022.159512
74. Srinivasan, M. (2019). Green synthesis and characterization of titanium dioxide nanoparticles (TiO_2 NPs) using Sesbania grandiflora and evaluation of toxicity in zebrafish embryos. *Process Biochemistry*, *80*, 197–202. https://doi.org/10.1016/j.procbio.2019.02.010
75. Srujana, S., Anjamma, M., Singh, B., Dhakar, R. C., Natarajan, S., R, Hechhu. (2022). A comprehensive study on the synthesis and characterization of TiO_2 nanoparticles using Aloe vera plant extract and their photocatalytic activity against MB Dye. *Adsorption*

Science & Technology. hindawi.com.

76. Subha, P. P., Jayaraj, M. K. (2015). Solar photocatalytic degradation of methyl orange dye using TiO_2 nanoparticles synthesised by sol–gel method in neutral medium. *Journal of Experimental Nanoscience*, *10*(14), 1106–1115. https://doi.org/10.1080/17458080.2014.969338
77. Subhapriya, S., Gomathipriya, P. (2018). Green synthesis of titanium dioxide (TiO_2) nanoparticles by Trigonella foenum-graecum extract and its antimicrobial properties. *Microbial Pathogenesis*, *116*(December 2017), 215–220. https://doi.org/10.1016/j.micpath.2018.01.027
78. Survase, A. A., Kanase, S. S. (2023). Green synthesis of TiO_2 nanospheres from isolated Aspergillus eucalypticola SLF1 and its multifunctionality in nanobioremediation of CI Reactive Blue 194 with antimicrobial and antioxidant activity. *Ceramics International 49*(10), 14964-14980. https://doi.org/10.1016/j.ceramint.2023.01.079.
79. ur Rehman, K., Zaman, U., Tahir, K., Khan, D., Khattak, N. S., Khan, S. U., Khan, W. U., Nazir, S., Bibi, R., Gul, R. (2022). A Coronopus didymus based eco-benign synthesis of Titanium dioxide nanoparticles (TiO_2 NPs) with enhanced photocatalytic and biomedical applications. *Inorganic Chemistry Communications*, *137*(August 2021), 109179. https://doi.org/10.1016/j.inoche.2021.109179
80. Safitri, V, Y, Santoni, A., Wellia, D, V., K. dan Safni. (2017). Degradation of Paracetamol by Photolysis Using C-N-codoped TiO_2. *Jurnal Ilmiah Kimia Department of Chemistry, Faculty of Mathematics and Natural Sciences, Universitas Jenderal Soedirman, Purwokerto, Indonesia*, *12*(2), 189–195. https://doi.org/10.20884/1.jm.2017.12.2.378
81. Sundar, V., Balasubramanian, B., Sivakumar, M., Chinnaraj S., Palani, V., Maluventhen, V., Kamyab, H., Chelliapan, S., Arumugam, M., D. P. Z. M. (2024). An eco-friendly synthesis of titanium oxide nanoparticles mediated from Syringodium isoetifolium and evaluate its biological activity and photocatalytic dye degradation. *Inorganic Chemistry Communications*, *161*(112125).
82. Viana, M. M., Soares, V. F., Mohallem, N. D. S. (2010). Synthesis and characterization of TiO_2 nanoparticles. *Ceramics International*, *36*(7), 2047–2053. https://doi.org/10.1016/j.ceramint.2010.04.006
83. Vishali, D., Manikandan, B., John, R., Murali, K. R. (2021). Degradation of methylene blue dye by tio_2 nanoparticles biologically synthesized using leaf extract of citrus aurantifolia. *Transactions on Electrical and Electronic Materials*, *22*(5), 622–629. https://doi.org/10.1007/s42341-020-00270-4
84. Wagutu, A. W., Yano, K., Sato, K., Park, E., Iso, Y., Isobe, T. (2019). Musa AAA and *Jatropha curcas* L. sap mediated TiO_2 nanoparticles: Synthesis and characterization. *Scientific African*, *6*, 0–9. https://doi.org/10.1016/j.sciaf.2019.e00203
85. Wellia, D. V., Syuadi, A. F., Rahma, R. M., Syafawi, A., Habibillah, M. R., Arief, S., Kurnia, K. A., Saepurahman, Kusumawati, Y., Saefumillah, A. (2024). Rind of *Aloe vera* (L.) Burm. f extract for the synthesis of titanium dioxide nanoparticles: Properties and application in model dye pollutant degradation. *Case Studies in Chemical and Environmental Engineering*, *9*(January), 100627. https://doi.org/10.1016/j.cscee.2024.100627
86. Zhang, C., Ren, X., Wang, K., Liang, X., Wu, Y., He, Y. (2024). Boosting piezocatalytic efficiency: Thin carbon layer-modified ZnO for superior rhodamine B degradation. *Ceramics International*, *50*(July), 43340–43344. https://doi.org/10.1016/j.ceramint.2024.08.068